TELKOMNIKA Indonesian Journal of Electrical Engineering
Vol.12, No.1, January 2014, pp. 618 ~ 626
DOI: http://dx.doi.org/10.11591/telkomnika.v12i1.3365

Multi-focus Image Fusion by SML in the Shearlet Subbands

Jianhua Liu, Jianguo Yang*, Beizhi Li
College of Mechanical Engineering, Donghua University, Shanghai, PR China
*Corresponding author, e-mail: jgyangm@163.com

Abstract

It is now widely acknowledged that traditional wavelets are not very effective in dealing with multidimensional signals containing distributed discontinuities. Shearlet Transform is a new discrete multiscale directional representation, which combines the power of multiscale methods with a unique ability to capture the geometry of multidimensional data and is optimally efficient in representing images containing edges. In this work, coefficients with greater Sum-Modified-Laplacian are selected to combine images when high-frequency and low-frequency Shearlet subbands of source images are compared. Numerical experiments demonstrate that the method base on Shearlet Transform and Sum-Modified-Laplacian is very competitive and better than other multi-scale geometric analysis tools in multifocus image fusion both in terms of objectives performance and objective criteria.

Keywords*: Shearlet, SML, Image fusion, NSCT*

1. Introduction

Image fusion can be defined as a process in which a new image is produced by integrating complementary, multi-temporal or multi-view information from a set of source images [1]. The resultant image acquired from image fusion technique is more informative and appropriate for the purposes of human visual perception and further image processing tasks such as segmentation, feature extraction and target recognition. Multi-focus image fusion is an important branch of this field. Due to the limited depth-of-focus of optical lenses in camera, it is often not possible to obtain an image that contains all relevant focused objects [2]. One way to overcome this problem is by using the multi-focus image fusion technique, through which several images with different focus points are combined to form a single image with all objects fully focused.

Recently, several multi-scale geometric analysis (MGA) tools, such as Ridgelet, Curvelet, and Contourlet transform have been developed. The MGA can take full advantage of the geometric regularity of image intrinsic structures and obtain the asymptotic optimal representation. As the latest MGA tool, Contourlet transform is a 'true' 2D sparse representation for images. It has the characteristics of localization multi-direction, and anisotropy. The Contourlet can give the asymptotic optimal representation of contours and has been successfully used in image fusion field [3]. In [4], a method for image fusion based on Contourlet transform and HiddenMarkov Tree Model is proposed. However, the Contourlet lack of shift-invariance and results in artifacts along the edges to some extend. Nonsubsampled Contourlet Transform (NSCT) [5] inherits the perfect properties of the Contourlet, and meanwhile possesses the shift-invariance. In [6], NSCT is used in image fusion to make full use of the characteristics of it. Shearlet [7] proposed by Easley et al., a new approach provided in 2005, equipped with a rich mathematical structure similar to wavelets, which are associated to a multiresolution analysis.

In this paper, a new multi-focus image fusion algorithm based on Shearlet and Sum-Modified-Laplacian (SML) [8] method was put forward in this study. The Shearlet Coefficients with greater SML are selected out to combine fused image when high-frequency and low-frequency Shearlet subbands of source images are compared. We name the proposed fusion method as Shearlet-SML method in this paper.

Received May 29, 2013; Revised July 15, 2013; Accepted August 11, 2013

2. Shearlet Transform

The basic theory of Shearlet transform is the theory of composite wavelet which provides a kind of effective method for multiscale analysis by the affine system. In dimension two, the affine system with the synthetic expansion character [9] form is as follow:

$$A_{AS}(\Psi)=\{\Psi_{j,k,l}(x)\}=\left|\det A\right|^{j/2}\Psi(S^{l}A^{j}x-k) \quad (1)$$

Where A, S are both 2×2 invertible matrices, $j,l\in Z,k\in Z^2$ and |det S|=1. The matrix Aj correlates with the scale of transform correlation. Sl correlates with the geometric scale. The element of AAS(Ψ) is called composite wavelet, if AAS(Ψ) meets the following form of Parseval tight frame: for $\forall f\in L^2(R^2)$, $\sum_{j,l,k}\left|\left\langle \psi_{j,l,k}\right\rangle\right|^2=\|f\|^2$.

When $\mathrm{A}=\mathrm{A}_0=\begin{pmatrix}a & 0\\ 0 & \sqrt{\mathrm{a}}\end{pmatrix}$ and $\mathrm{S}=\mathrm{S}_0=\begin{pmatrix}1 & 1\\ 0 & 1\end{pmatrix}$, the transform is called a Shearlet Transformt. A0 is anisotropic dilation matrix. S0 is shear matrix.

For $\forall\xi=(\xi_1,\xi_2)\in R$ and $\xi_1\neq 0$, let $\hat{\Psi}^{(0)}(\xi)$ be given by $\hat{\Psi}^{(0)}(\xi)=\hat{\Psi}^{(0)}(\xi_1,\xi_2)=\hat{\Psi}_1(\xi_1)\hat{\Psi}_2(\xi_1/\xi_2)$. Where $\hat{\Psi}_1\in C^{\infty}(R)$ is wavelet and $\hat{\Psi}_2\in C^{\infty}(R)$, supp $\hat{\Psi}_1\subset[-1/2,-1/16]\cup[1/16,1/2]$ and $\hat{\Psi}_2\subset[-1,1]$. This implies $\hat{\Psi}^{(0)}\in C^{\infty}(R)$, and supp $\hat{\Psi}^{(0)}\in[-1/2,1/2]$.

In addition, we assume that

$$\sum_{j\geq 0}\left|\hat{\Psi}(2^{-2j}\omega)\right|^2=1,\ |\omega|\geq 1/8 \quad (2)$$

And for $\forall j\geq 0$,

$$\sum_{l=-2^j}^{2^j-1}\left|\hat{\Psi}(2^{-2j}\omega-l)\right|^2=1,\qquad |\omega|\leq 1 \quad (3)$$

Thus, it can be concluded from formula (2) and formula (3) that for $\forall(\xi_1,\xi_2)\in D_0$,

$$\sum_{j\geq 0}\sum_{l=-2^j}^{2^j-1}\left|\hat{\Psi}^{(0)}(\xi A_0^{-j}S_0^{-l})\right|^2=\sum_{j\geq 0}\sum_{l=-2^j}^{2^j-1}\left|\hat{\Psi}_1(2^{-2j}\xi_1)\right|^2\left|\hat{\Psi}_2(2^j\frac{\xi_2}{\xi_1}-l)\right|^2=1.$$

where $D_0=\left\{(\xi_1,\xi_2)\in\hat{R}^2:\ |\xi_1|\geq 1/8,|\xi_2|\leq 1\right\}$, the function $\left\{\hat{\Psi}^{(0)}\left(\xi\mathrm{A}_0^{-\mathrm{j}}\mathrm{S}_0^{-\mathrm{j}}\right)\right\}$ forms a tiling of D0 which is shown in Fig.1. ξ_1,ξ_2 are the coordinate axes of the Shearlet transform in frequency domain. Because of the supporting conditions on $\hat{\Psi}_1$ and $\hat{\Psi}_2$, the function $\Psi_{j,l,k}$ has the following domain support: $\hat{\Psi}_1^{j,k,l(0)}\subset(\xi_1,\xi_2):\xi_1\in[-2^{2j-1},-2^{2j-4}]\cup[2^{2j-4},2^{2j-1}],\left|\frac{\xi_2}{\xi_1}+l2^{-j}\right|\leq 2^{-j}$.

That is to say, $\hat{\Psi}_{j,l,k}$ is support on a pair of trapezoids, which the size is approximately $2^{2j}\times 2^{j}$ and oriented along lines of slope $l2^{-j}$. j is the scale of the Shearlet transform. This is shown in the Figure 2.

Similarly, we can construct a Parseval frame $L^2(D_1)^{\vee}$ where D_1 is the vertical cone [10].

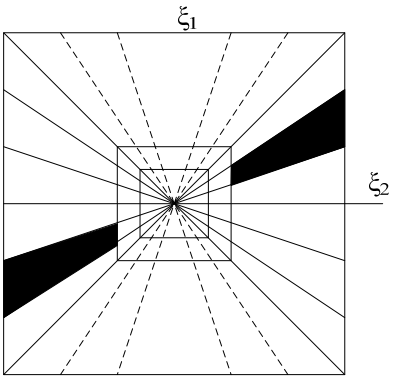

Figure 1. The tiling of the Shearlet in Frequency domain

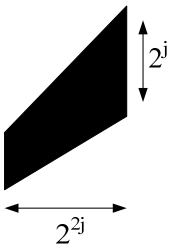

Figure 2. The parabola scale of the Shearlet transform

3. Sum of the Modified Laplacian

A focus measure should be defined which is a maximum for the best focused image and it should decrease as the defocus increases. Therefore, in the field of multifocus image fusion, the focused image areas of the source images must produce maximum focus measures, the defocused areas must produce minimum focus measures in contrast [11]. Let I(*i*,*j*) be the gray level intensity of pixel (*i*,*j*) for image I.

The ML (Modified Laplacian) takes the absolute values of the second derivatives in the Laplacian to avoid the cancellation of second derivatives in the horizontal and vertical directions that have opposite signs. The ML is defined as follows:

$$\begin{aligned} \mathrm{ML}^{l,\ k}(\mathrm{i},\mathrm{j}) = &\left|2I^{l,k}(i,j) - I^{l,k}(i-step,j) - I^{l,k}(i+step,j)\right| \\ &+ \left|2I^{l,k}(i,j) - I^{l,k}(i,j-step) - I^{l,k}(i,j+step)\right| \end{aligned} \tag{4}$$

Where the parameters k(*i*,*j*) is the coefficient located at (*i*,*j*) in the *l*-th scale and *k*-th direction subband.

In order to accommodate for possible variations in the size of texture elements, Nayar (1994) used a variable spacing (step) between the pixels to compute ML. In this paper 'step' always equals to 1. The focus measure at a point (*i*,*j*) is computed as the SML [12] (Sum of the Modified Laplacian), in a window around the point:

$$\mathrm{SML}^{l,\ k}(\mathrm{i},\mathrm{j}) = \sum_{m=-M}^{M}\sum_{n=-N}^{N}[\mathrm{ML}^{\mathrm{l,k}}(i+m,j+n)]^2 \tag{5}$$

Where the parameters M and N determine the window with size (2M+1)×(2N+1) is used to compute the focus measurement.

4. The Proposed Fusion Algorithm

The image fusion framework based on shearlets is shown in Fig. 3. The following steps of image fusion are adopted.

Step 0: The original images A and B taking part in the fusion are geometrically registered to each other.

Step 1: Transform the original images A and B using Shearlets, respectively, into one low-frequency sub-image and a series of high-frequency sub-images at *l* levels and *k* directions via Shearlets. Let $Sh_A^{l,k}(i,j)$ and $Sh_B^{l,k}(i,j)$ separately denote a series of coefficients of the original images A and B, decomposed to some level and direction via Shearlet Transform.

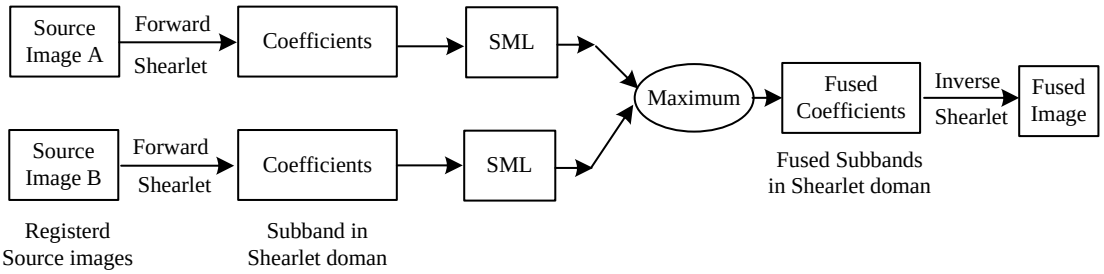

Figure. 3 Schematic diagram of Shearlet-SML fusion algorithm

Step 3: Calculate the $SML_A^{l,k}$ and $SML_B^{l,k}$ value of every Shearlet coefficients subbandof the images including the high frequency coefficients and low frequency coefficients

Step 4: Obtain the fuse-decision map by the following formula (6). And select the coefficients by (7), which mean that coefficients with large SML value are selected as coefficients of the fused image.

$$\mathrm{Map}^{l,k}(i,j) = \begin{cases} 1 & \mathrm{SML}_A^{l,k}(i,j) \geq \mathrm{SML}_B^{l,k}(i,j) \\ 0 & \mathrm{SML}_A^{l,k}(i,j) < \mathrm{SML}_B^{l,k}(i,j) \end{cases} \quad (6)$$

$$Sh_F^{l,k}(i,j) = \begin{cases} SH_A^{l,k}(i,j) & if\ \mathrm{Map}^{l,k}(i,j) = 1 \\ SH_B^{l,k}(i,j) & if\ \mathrm{Map}^{l,k}(i,j) = 0 \end{cases} \quad (7)$$

Where $Sh_F^{l,k}(i,j)$, $Sh_A^{l,k}(i,j)$ and $Sh_B^{l,k}(i,j)$ are the coefficients of the fused image F, A and B respectively.

Step 5: Reconstruct the new fusion image based on the new fused Shearlet coefficients by taking an inverse Shearlet transform.

5. Evaluation Criterion

For comparison the fusion results by different method, two objective criteria are used to compare the fusion results.

The first criterion is the mutual information (MI) metric proposed by Pile [13]. The MI metric is employed here to objectively evaluate the performance of the PCNN methods in four different multiscale decomposition domains. This metric can demonstrate how much information the fused image conveys about the reference image [14]. Thus, the higher the MI is, the better the result is. The MI is defined as:

$$MI(x_R; x_F) = \sum_{u=1}^{L}\sum_{v=1}^{L} h_{R,F}(u,v)\log_2 \frac{h_{R,F}(u,v)}{h_R(u)h_F(v)} \quad (8)$$

Where x_R and x_F denote the reference image and fused image, respectively, $h_{R,F}$ is the joint gray level histogram of x_R and x_F , h_R and h_F are the normalized gray level histograms of x_R and x_F, and L is the number of bins.

The second criterion is the $Q^{AB/F}$ metric, proposed by Xydeas and Petrovic in [15], which considers the amount of edge information transferred from the input images to the fused images. This method uses a Sobel edge detector to calculate the strength and orientation information at each pixel in both source image A, image B and fused image F.

The Sobel edge operator is applied to yield the edge strength g(n,m) and orientation α(n,m) information for each pixel as [17]:

$$g_A(n,m) = \sqrt{s_A^x(n,m)^2 + s_A^y(n,m)^2} \quad (9)$$

$$\alpha_A(n,m) = \tan^{-1}\left(\frac{s_A^y(n,m)}{s_A^x(n,m)}\right) \quad (10)$$

Where $s_A^x(n,m)$ and $s_A^y(n,m)$ are the output of the horizontal and vertical Sobel templates centered on pixel $p_A(n,m)$ and convolved with the corresponding pixels of image A. The relative strength and orientation values of an input image A with respect to F are formed as:

$$\left(G_{n,m}^{AF}, A_{n,m}^{AF}\right) = \left(\left(\frac{g_{n,m}^F}{g_{n,m}^A}\right)^M, 1 - \frac{\left|\alpha_A(n,m) - \alpha_F(n,m)\right|}{\pi/2}\right)$$

Where $M = \begin{cases} 1 & if \quad g_A(n,m) > g_F(n,m) \\ -1 & otherwise \end{cases}$.

Edge information preservation values are then defined as: $Q_{n,m}^{AF} = \Gamma_g \Gamma_\alpha (1 + e^{k_g (G_{n,m}^{AF} - \sigma_g)})^{-1} (1 + e^{k_\alpha (A_{n,m}^{AF} - \sigma_\alpha)})^{-1}$

Finally, the QAB/F is defined as:

$$Q^{AB/F} = \frac{\sum_{\forall n,m} Q_{n,m}^{AF} w_{n,m}^A + Q_{n,m}^{AF} w_{n,m}^B}{\sum_{\forall n,m} w_{n,m}^A + w_{n,m}^B} \quad (11)$$

Which evaluates the sum of edge information preservation values for both inputs Q^{AF} and Q^{BF} weighted by local importance perceptual factors w^A and w^B, we defined $w^A(n,m) = \left[g_A(n,m)\right]^T$ and $w^B(n,m) = \left[g_B(n,m)\right]^T$. T is a constant. For the 'ideal fusion', $Q^{AB/F}$=1.

6. Experiments

The two pairs of images showed in Figure 4 and Figure 5 are used as source images to be fused in multi-focus images. In this paper, we compare this method of Shearlet-SML with the other method such as the CS-SFLCT-SML proposed by Qu and the NSCT method based on the SML. In the direction of the filter decomposition, the decomposition parameter is set as [2,3,3,4,4]. The shift distance are set as M=N=[-1,-2,-4,-8,1,2,4,8]. The M is the shift distance in the *x* axis and the N is the shift distance in the *y* axis.

In NSCT decomposition, [2,3,3,4,4] is used as the vector of numbers of directional filter bank decomposition levels at each pyramidal level (from coarse to fine scale). The filter name for the directional decomposition step is 'pkva'. The name of the pyramid 2D filters is 'maxflat'.

In the Shearlet transform, the filter 'pyr' is used as the filter for the Laplacian Pyramid. [2,3,3,4,4] is used as a vector such that dcomp(i) indicates that the i-th decomposition level has 2^decomp(i) directions. That is to say, the levels of the Shearlet, NSCT and SFLCT decomposition are 5.

After the above three multiscale transform decomposition of the image A and image B, the SML fusion rule is to applied to each subband included the low frequency and high frequency. The experiment shows the SML fusion rule in the every subband is better than the mean coefficient method and the max coefficient method in low frequency subband. The experiment results fusing the image by the SML rule are shown in the Figure 4 and Figure 5.

The fusion results of fusing image 'Clock' are shown in Figure 4(c)–(e) with CS-SLCT, NSCT and Shearlet transform by SML. We see that using shearlets we obtained a fusion image in which the left clock is clearer than with the other methods. Figure 4 (g)–(h) show the difference between fused images by above three methods with the Figure 4 (a). It indicates that Shearlet-SML extracts characteristics better than the other two methods for multi-focus images fusion examples.

The fusion results of the image 'Pepsi' are shown in Figure 5(c)–(e) with CS-SLCT, NSCT and Shearlet transform by SML. Figure 5 (g)–(h) show the difference between fused images by above three methods with the Figure 5 (a).

From Figure 4 and Figure 5, We can see that image fusing using Shearlets can obtain a fusion image, on which the fusion image can be seen clearly than other method. It indicates that Shearlet-SML extracts the better features than the other two methods in 'Pepsi' and 'Clock' images fusion.

The MI values of the four different methods in Figure 4 and Figure 5, are calculated and shown in Table 1. It can be seen from Tab. 1 that the MI value of the proposed method is the largest in the three methods, and the MI value of the CS-SFLCT method is the smallest. The results presented in this example can demonstrate that our approach can fuse the multi-focus images while retaining much more information than that of the other two methods.

Table 1. Performance of fusion by SML in different transform coefficients

Images	Criteria	CS-SFLCT+SML	NSCT+SML	Shearlet+SML
Clock	MI	6.5898	7.1168	7.2130
	$Q^{AB/F}$	0.6651	0.6767	0.6834
Pepsi	MI	6.6714	7.0627	7.2290
	$Q^{AB/F}$	0.7665	0.7711	0.7760

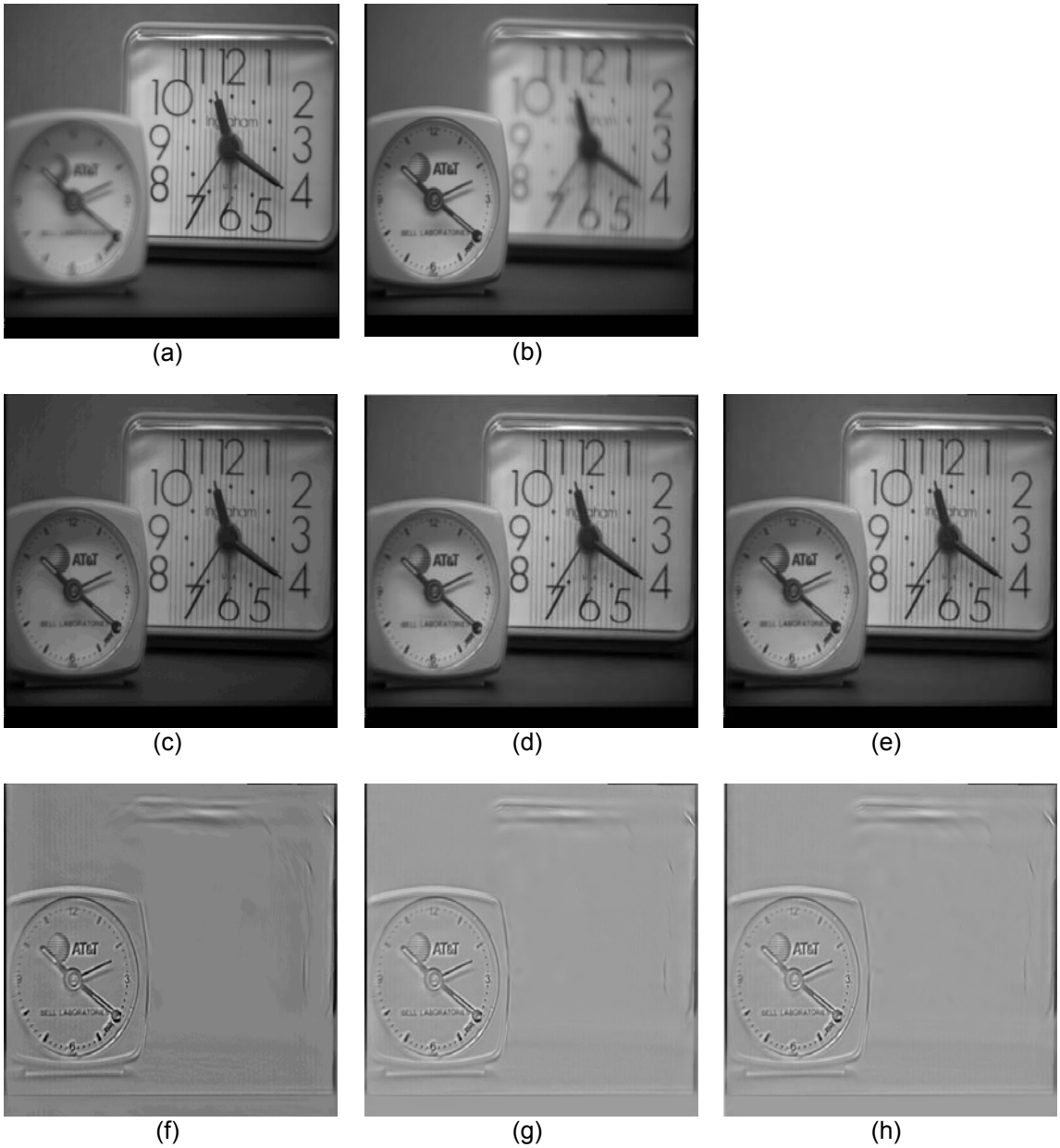

Figure 4. The fusion results of 'Clock' image by SML in different transform coefficients (a) ClockA focused on the left; (b) ClockB focused on the right; (c)-(e) Fused image by CS-SFLCT method, NSCT, Shearlet; (f) Difference image between (c) and (a); (g) Difference image between (d) and (a); (h) Difference image between (e) and (a)

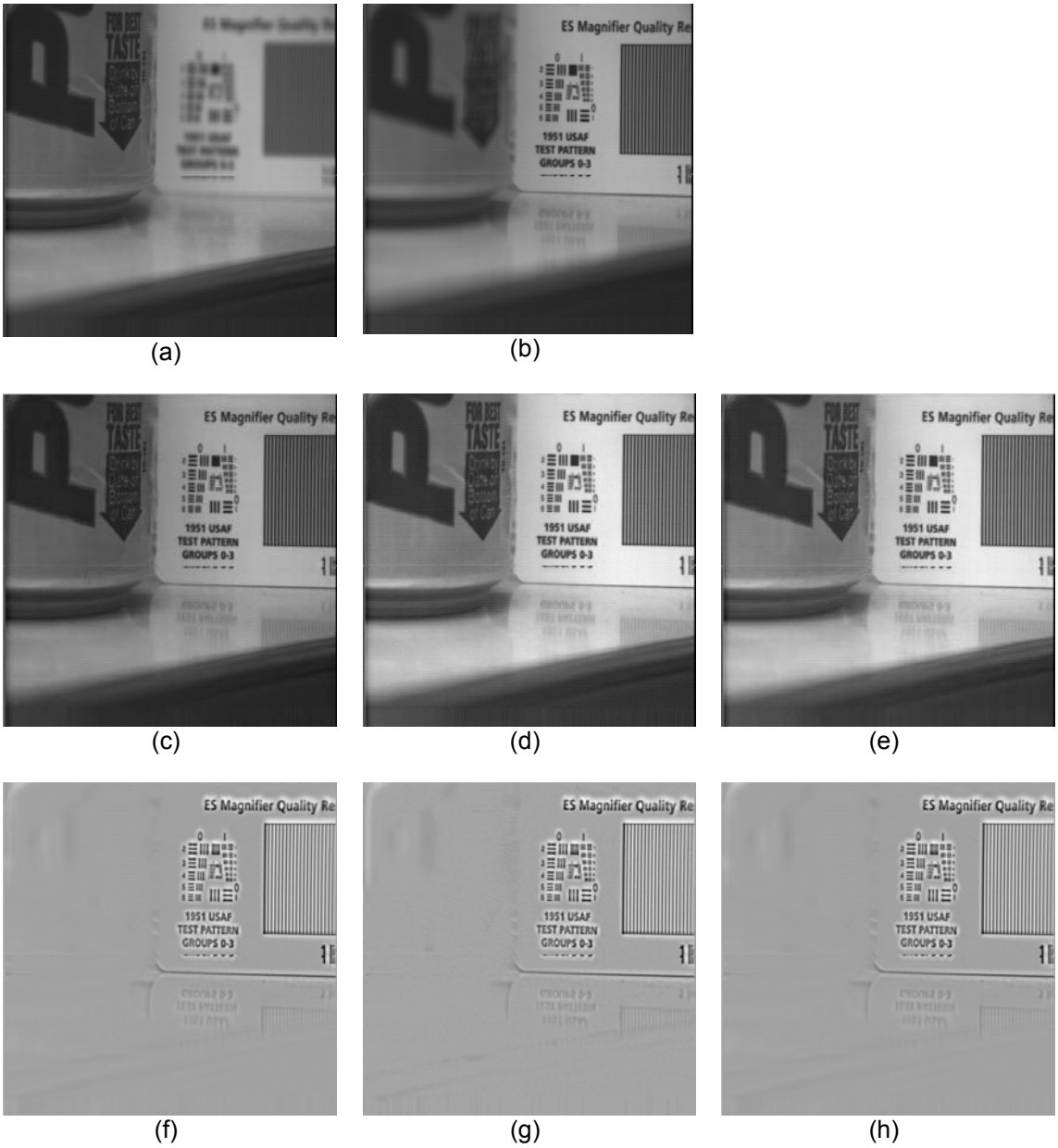

Figure 5. The fusion results of 'Pepsi' image by SML in different transform coefficients (a) Pepsi focused on the left; (b) Pepsi focused on the right; (c)-(e) Fused image by CS-SFLCT, NSCT, Shearlet; (f) Difference image between (c) and (a); (g) Difference image between (d) and (a); (h) Difference image between (e) and (a)

7. Conclusion

The main advantage of Shearlets is that it can be studied within the framework of a generalized Multi-resolution analysis and with directional subdivision schemes generalizing those of traditional wavelets. The Shearlet is a 'true' two-dimensional MGA tool that captures intrinsic geometrical structure, and it has been shown to be successful for many tasks in image processing such as image denoising, sparse image representation and edge detection. Furthermore, the method can yield more accurate reconstruction of images compared to NSCT and CS-SFLCT. In this paper, we presented a new fusion method based on the combination of the Shearlet transform and the SML. In this method, a SML-based fusion rule was employed to make a decision on selecting the Shearlet coefficients for high frequency and low frequency

subbands. The results of experiments demonstrate the effectiveness of our proposed method by the objective criteria and the visual appearance.

References

[1] Gabarda, Salvador, Cristóbal, Gabriel. On the use of a joint spatial-frequency representation for the fusion of multi-focus images. *Pattern Recognition Letters*. 2005; 26(16): 2572-2578.

[2] Yi Chai, Huafeng Li, Zhaofei Li. Multifocus image fusion scheme using focused region detection and multiresolution. *Optics Communications*. 2011; 284: 4376-4389.

[3] Directional multiscale modeling of images using the contourlet transform Po, Duncan DY. (Department of Electrical and Computer Engineering, University of Illinois at Urbana-Champaign, Urbana, IL 61801, United States); Do, Minh N. Source: IEEE Transactions on Image Processing. 2006; 15(6): 1610-1620.

[4] LIU Kun, GUO Lei, CHEN Jingsong. Image Fusion Algorithm Based on Contourlet Domain HiddenMarkov Tree Models. *ACTA Phot on Ica Sinica*. 2010; 39(8).

[5] JP Zhou, AL da Cunha, MN Do. Nonsubsampled contourlet transform: construction and application in enhancement. in: *IEEE International Conference on Image Processing*, Genoa, Italy. 2005: 469–476.

[6] Zhang Qiang, Guo Baolong. Multifocus image fusions using the nonsubsampled contourlet transform. *Signal Processing*. 2009; 89(7): 1334-1346.

[7] Easley GL, Demetrio, Lim Wang Q. Sparse directional image representations using the discrete Shearlet transform. *Applied and Computational Harmonic Analysis*. 2008; 25(1): 25-46.

[8] Qu Xiaobo, Yan Jingwen, Yang Guide. Sum-modified-Laplacian-based Multifocus Image Fusion Method in Sharp Frequency Localized Contourlet Transform Domain. *Optics and Precision Engineering*. 2009; 17(5): 1203-1202.

[9] Peng Geng, Zhengyou Wang, Zhigang Zhang and Zhong Xiao. Image fusion by pulse couple neural network with shearlet. Opt. Eng. 51(6), 067005 (Jun 06, 2012). http://dx.doi.org/10.1117/1.OE.51.6.067005

[10] Easley, Glenn R, Labate, Demetrio, Colonna, Flavia. Shearlet-based total variation diffusion for denoising. *IEEE Transactions on Image Processing*. 2009; 18(2): 260-268.

[11] Nayar SK, Nakagawa Y. Shape from focus. *IEEE Transactions on Pattern Analysis and Machine Intelligence*. 1994; 16(8): 824–831.

[12] Stanciu, Stefan G, Drăgulinescu, Marin Stanciu, George A. Sum-modified-Laplacian Fusion Methods experimented on image stacks of photonic quantum ring laser devices collected by confocal scanning laser microscopy. UPB Scientific Bulletin, Series A: Applied Mathematics and Physics. 2011; 73(2) 139-146.

[13] G Piella. A general framework for multiresolution image fusion: from pixels to regions. *Information Fusion*. 2003; 4(4): 259-280.

[14] Yang Yong, Park Dongsun, Huang Shuying, Rao Nini. Medical image fusion via an effective wavelet-based approach. *Eurasip Journal on Advances in Signal Processing*. 2010; 2010.

[15] Xydeas CS, Petrovic V. Objective image fusion performance measure. *Electronics Letters*. 2000; 36(4) 308-309.